A MULTI-PERSPECTIVE EXAMINATION OF THE PHYSICS OF ELECTROMAGNETIC RADIATION

E. K. Miller
3225 Calle Celestial
Santa Fe, NM 87501-9613
505-820-7371, ekmiller@prodigy.net

G. J. Burke
Lawrence Livermore National Laboratory
PO Box 808, Livermore, CA 94550
925-422-8414, burke2@llnl.gov

ABSTRACT
Three different perspectives of electromagnetic radiation are presented here. The first employs the electric-field kink model, the second is based on a technique called FARS (Far-field Analysis of Radiation Sources), and the third uses time-domain solutions obtained from the TWTD (Thin-Wire Time Domain) model. The kink model demonstrates qualitatively that radiation is produced by "wriggling" a charge. The latter two provide more quantitative results, showing that radiation for a straight dipole can come not only from the source region and ends but also from along its length.

1. INTRODUCTION

Perhaps the most fundamental property of electromagnetic (EM) fields is that of radiation, in the absence of which the world would be a much different place. Radiation, of course, is the means by which EM energy leaves a localized source to propagate in space, attenuating with distance, r, in three dimensions as $1/r^2$. The analytical foundation for EM fields is the long-corroborated Maxwell equations that provide the basis for understanding phenomena ranging from radar scattering to satellite communications. The Maxwell equations also can be manipulated to show that a necessary and sufficient condition to generate EM radiation is the presence of accelerated charge [1]. Explicit consideration of charge acceleration is normally not needed, however, to analyze the kinds of boundary-value (BV) problems that arise in engineering EM. This can be contrasted when dealing with moving charge in free space such as designing charged-particle accelerators, for example. This is because the role of charge acceleration in causing a radiation field is implicit in the source (current and charge) terms in the Maxwell equations for the former problem, whereas for the latter the mechanical motion of physical charges must also be taken into account. Determining the charge behavior explicitly as part of solving a BV problem, or inferring it from the radiation fields that are produced, would be useful for design, as well as insightful from a physics' viewpoint. The possibility of establishing a quantitative connection between EM power flow in the far field and where that power originates from over the surface of an antenna is the focus of the following discussion.

The prototype engineering EM BV problem involves finding the fields external to an object assumed to be a perfect electric conductor (PEC) on whose surface the total tangential field is identically zero, while the tangential component of the total magnetic field is terminated by the conduction current that flows on this surface. The physical behavior and properties of electrons inside an actual metal object are not relevant to this approach since the assumption of perfect conductivity is equivalent to assuming that the surface charges redistribute instantaneously to accommodate changes in the external field, thereby maintaining an identically zero tangential electric field at the object's surface. In a physics' context, this amounts to dealing with fictitious charges possessing infinite mobility and/or zero mass. While this approach simplifies the solution of such problems, the connection between charge acceleration and radiation fields tends to be obscured. Never-the-less, the assumption of perfect conductivity leads to solutions that conform to experimental measurements within experimental error for problems where the surface impedance of the object is effectively zero, i.e., for good conductors. Why this can be so when the actual charge in a metal is comprised of electrons which have neither zero mass nor infinite mobility will be discussed further in Section 3.

Although dealing with accelerated charge is not necessary when using the typical engineering EM approach just considered, implicit in that solution must be the effects of such acceleration if the correct radiated fields are to be obtained. And, since the radiated field is caused by the accelerated charge, knowledge about where the radiated power comes from over the surface of a body on a per-unit-length or -area basis should yield information about where the charge is accelerated, and vice versa. It is this particular issue that is discussed in the following, with attention limited to thin-wire objects. The specific issue to be addressed here is to ask if it can be determined quantitatively where the radiation comes from for an object as simple as a straight, thin-wire antenna. This seemingly simple question is not without controversy, as some in the electromagnetics community feel that quantitatively establishing where the radiation originates is not possible and, further, that this is not even a sensible question to ask. It is hoped that the results presented below will factually reject that position. It should be emphasized that while the numerical results to be presented, derived from a well-validated computational model, can be regarded as being correct for the problems investigat-

ed, it is the interpretation thereof that might be debated. Before presenting these numerical results, some preliminary observations based on a semi-quantitative model of radiation will be discussed, that of the electric-field (or E-field) kink model.

2. A SEMI-QUANTITATIVE APPROACH TO RADIATION USING THE E-FIELD KINK MODEL

The purpose of the brief discussion that follows is to demonstrate that one of the most fundamental properties of EM fields, the radiation and propagation of power through space, can be explained without resorting to complicated mathematics. This demonstration depends on the two basic observations that the propagation speed of EM fields is finite, and that electric field lines in source-free regions are continuous. That the kink model does not seem to be widely known in the engineering community is unfortunate. The authors first learned of it in connection with the Cabrera program [2] from which the results in this section were generated. An extensive discussion of the procedure, though not denoted as the E-field kink model, is given by Smith [3] who cites several references to it, the first being Thomson [4]. It's not clear whether an analogous approach using the magnetic field might be derived.

That radiation occurs as a result of charge acceleration can be demonstrated by putting these two facts together. Consider a stationary, isolated charge at the origin, O, of a rectangular coordinate system, whose electric field lines therefore lie along radii terminating at O, as shown in Fig. 1a in a plane containing the x-axis. If the charge is abruptly accelerated to a velocity v = 0.3c along the +x axis, then after a time $t = t_1$ has passed the field lines will be as shown in Fig. 1b. An observer at a point $R = \sqrt{(x^2 + y^2 + z^2)}$ won't be aware of the charge movement until a time t = R/c has passed, at which time the electric field at the observer's position will change. This change occurs because the E-field lines that terminated initially on the charge at the origin must "shift" over time with the changing charge position, a process that is not instantaneous because c has a finite value. Also, because of the continuity in the E-field lines, the outer part of a given line will continue to point to the origin while that part near the charge will point to its changing location. Thus, to remain continuous, the old and new field lines must be joined by a line segment (or kink) that is parallel to neither, but which lies along the circumference of the sphere (a circle in this two-dimensional plot) defined by R = ct and which moves outward at the speed of light. These kinks constitute the electric components of an electromagnetic radiation field, accompanied by magnetic-field components as well, which are not shown here. If the charge is abruptly stopped at time t_1, a second spherical surface of E-field kinks is formed as shown in Fig. 1c at a time t_2 later. This new surface propagates outward from the position $x = vt_1$ about which it has expanded to the radius $R = ct_2$ while the original radiation pulse has further expanded to a radius $R = c(t_1 + t_2) = ct_3$. Note that although the two acceleration impulses are opposite in direction, they are equal so that the same energy will be contained in the respective radiation fields they produce.

There are some other interesting phenomena to observe in Fig. 1. Note that the E-field lines joining the two kinks continue to move in the +x direction at the speed v to continue pointing at the location where the charge would have be had it not been stopped. In addition, observe that the kink portions lengthen as their respective spheres propagate further away from their origins, indicating a decreasing value of their electric fields in proportion to 1/r. Finally, note that the distance between the acceleration and deceleration kinks in Fig. 1c is shorter in the +x direction than in the -x direction. This, of course, demonstrates the well-known Doppler shift exhibited by a moving source of electromagnetic or acoustic energy.

2.1 Some Simple Charge Motions that Produce Radiation

The radiation kink model, although not useful for solving boundary-value problems in EM, is never-the-less very helpful for illustrating various kinds of radiation phenomena. A computer program based on the kink model was developed at Stanford University about 1985 by Cabrera [2]. This program develops a series of E-field plots for a point charge undergoing certain kinds of motion selected by the user. These plots can then be viewed as a movie to display the evolution of the field as a function of time in a manner similar to a continuous "film loop." Some sample plots made by that program are presented here to show how simple the radiation process actually is, in contrast with the mathematical complexity needed to describe it rigorously. In the results shown, time advances in proceeding from part (a) to (b) to (c) of each figure, with all obtained from Cabrera's program [2].

2.1.1 A Charge Given a Continuous Push--An abrupt push, as illustrated in Fig. 1, is perhaps the simplest kind of radiation-producing acceleration to visualize, but suppose instead that a charge is continuously accelerated. While relativity theory shows that the charge's final speed can't exceed that of light, its speed can approach c, increasing in mass as it does so. As seen in Fig. 2 where the final speed is 0.99c, the radiation has the appearance of an EM shock-wave with a zone of nearly overlapping field lines which is most concentrated in the forward direction. This kind of radiation is what would be associated with a linear particle accelerator where charged particles are accelerated to speeds approaching c over extended distances.

2.1.2 A Charge Moving at Constant Speed Around a Circle--Results are shown in Fig. 3 for a charge moving around a circle at a constant speed of 0.9c. There the strongest radiation field can be seen as a spiral of coalescing field lines synchronized with the motion of the

charge around the circle. This is the kind of radiation produced in circular particle accelerators, and is known as "Synchrotron" radiation, or alternatively, searchlight radiation The radiation takes place continuously here since the charge is constantly inwardly accelerated as it moves around the circular path, in contrast with the linear acceleration of the previous examples.

2.1.3 A Charge Moving at Constant Speed Around a Square--Results for a charge moving at a constant speed of 0.5c around a square path are shown in Fig. 4. This kind of charge motion can be especially illuminating since the radiation occurs in a series of pulses as the charge moves around each right-angle corner of the square. During the time the charge moves along the straight side of the square, there is no radiation, but a circular radiation field can be seen centered on each corner as the charge changes direction there.

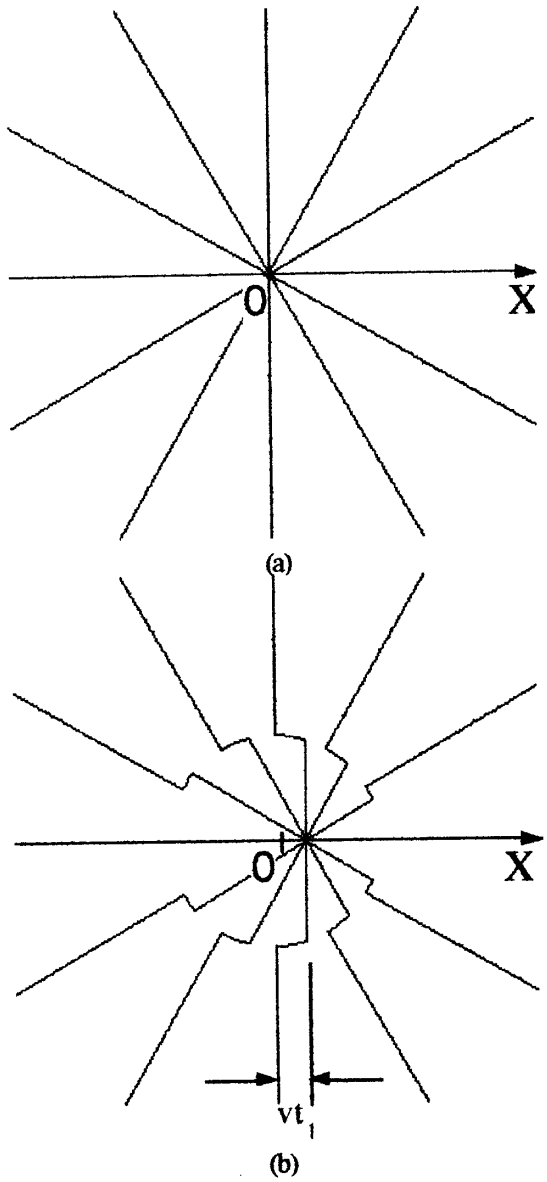

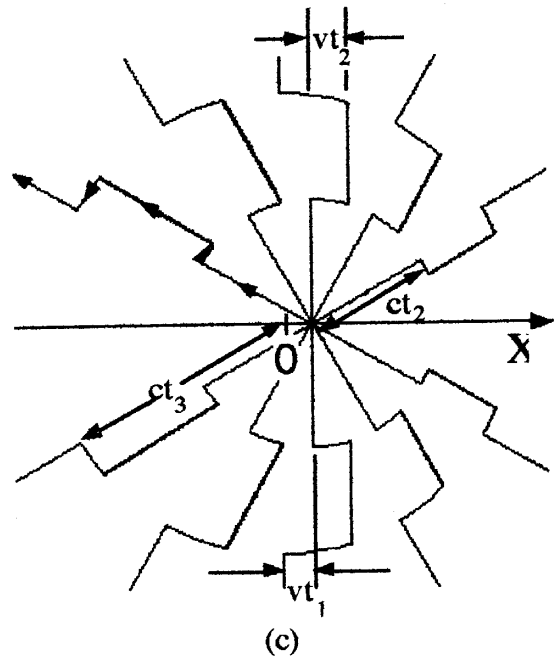

Figure 1. Depiction of the E-field lines for an initially stationary charge (a) that's abruptly accelerated from the origin to a speed v = 0.3c to then coast along the positive x-axis until time t_1 (b) when it is abruptly stopped (c).

Information about the changed charge positions propagates outward from its old and new positions at the speed of light. This is shown by the circular line segments joining the original field lines and those moving with the charge (b) and the moving field lines and those that terminate at the new stationary position (c). The direction of the radiated field caused by charge acceleration is opposite that due to deceleration as can be seen by the reversed directions of the kinks on the field line with the arrows in this plot.

2.1.4 A Charge Undergoing Oscillatory Motion--The kind of oscillatory motion considered here is the one most relevant to frequency-domain antennas, the charge here moving back-and-forth along a straight line with speed that varies as $V\cos(\omega t) = V\cos(2\pi f)$ with V = 0.5c. This is not exactly analogous to how the charge motion varies on an actual wire antenna, but it suffices to illustrate the production of a time-harmonic radiation field as shown in Fig. 5. The radiation field is seen to be oscillatory in space, and therefore in time as well at a fixed observation point, as the wave propagates by.

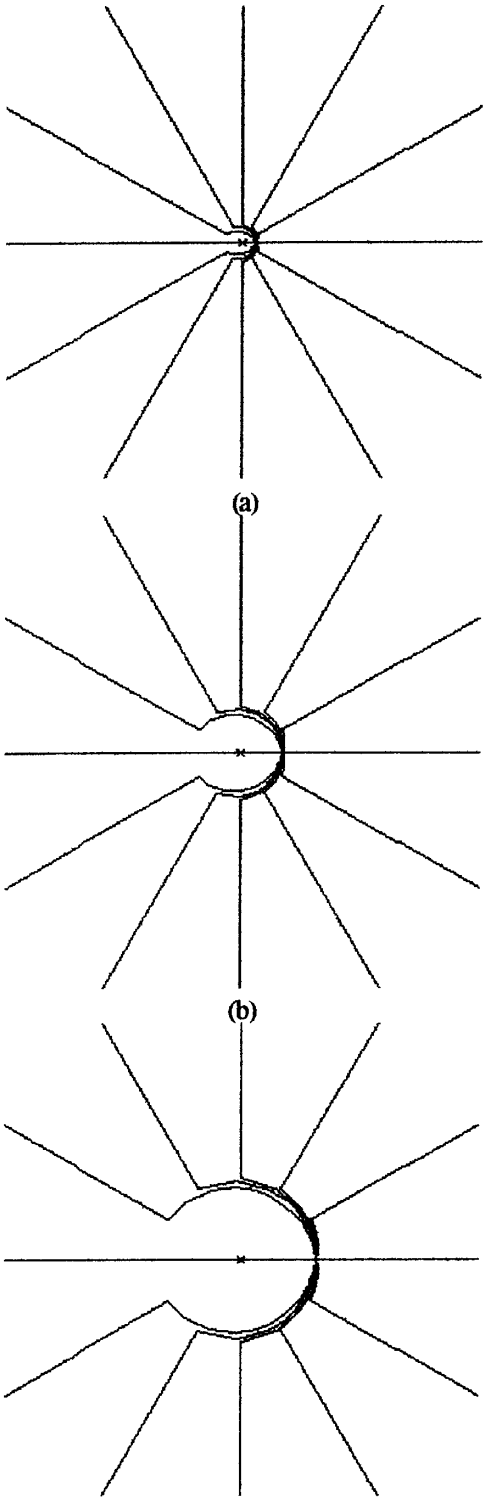

Figure 2. E-field lines for a charge accelerated to 0.99c by a constant force. Because its speed is so near c where an effect due to relativity arises, the field lines at the charge are concentrated in a small angular sector about the perpendicular, creating an EM shock wave. Note that each plot is centered on the moving charge.

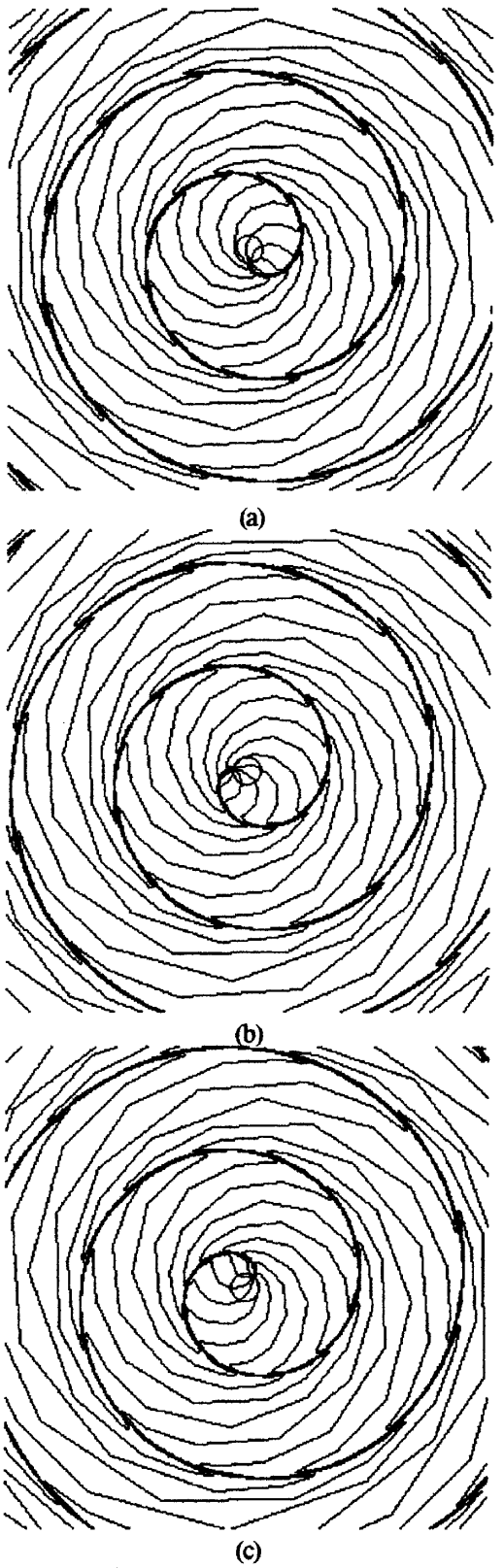

Figure 3. E-field lines for a charge moving in a circular path at a speed 0.9c. High values of electric field are indicated by the dark bands in this figure, producing an effect called Synchotron radiation.

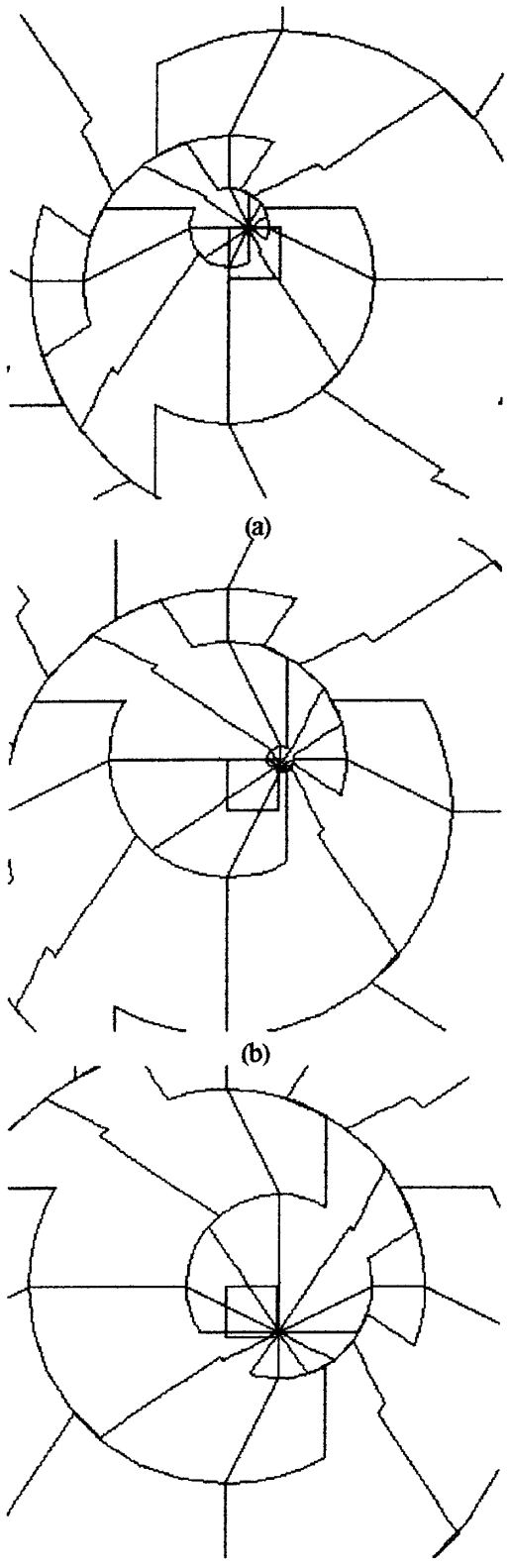

Figure 4. E-field lines for a charge moving around a square path at a constant speed of 0.5c. The charge produces an expanding circle of radiation as it goes around each of the right-angle corners of the square.

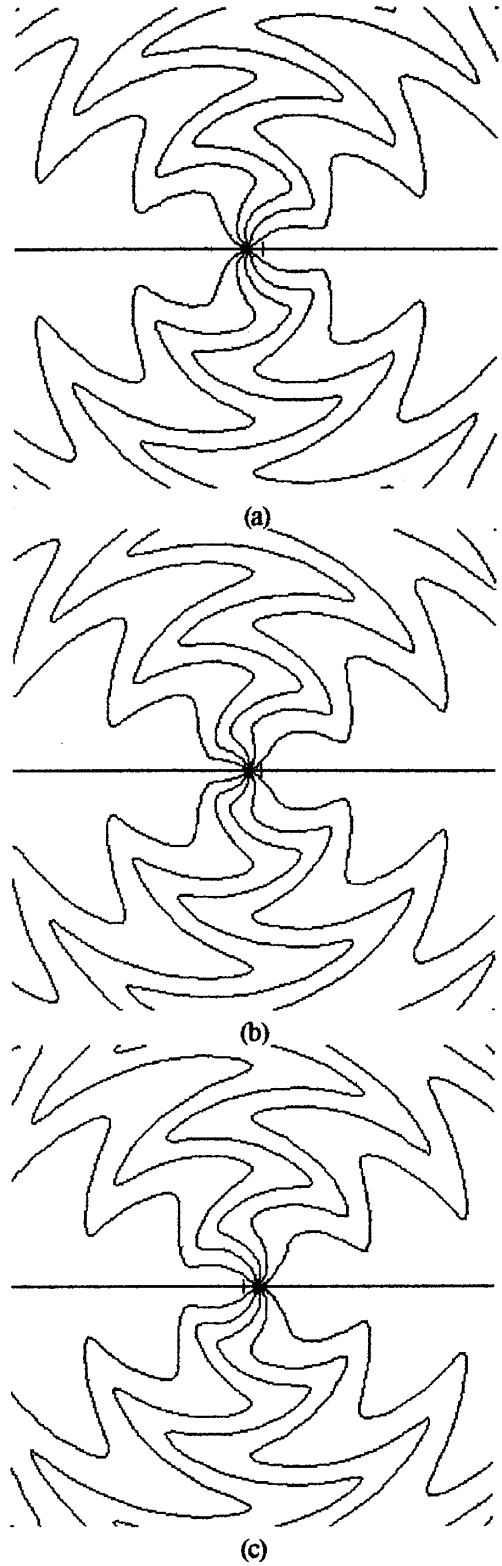

Figure 5. The E-field lines about a point charge undergoing oscillatory motion along a straight line with a maximum speed of 0.5c. Generation of outward propagating, time-harmonic waves is clearly discernible, in a fashion somewhat analogous to how an actual wire antenna works.

2.2 Some Observations

At this point it's appropriate to point out that a kink model demonstrates that EM radiation is essentially produced by "wriggling" a charge so as to wriggle its E-field lines. As can be seen in Fig. 5, the outward-propagating waves carried by a line of electric field is tantalizingly similar to the waves caused on a rope tied on one end by wriggling the other end. This analogy is not entirely superficial since both waves are transverse. Also, a field line in the direction of the wriggling charge motion carries no wave and neither does a rope when its end is pushed or pulled on. Thus, any time a charge, or a conduction current which after all is comprised of moving charges, is wriggled, radiation can be expected. The kink model, it should be noted, doesn't include any explicit consideration of the energy needed to make physical charges move in the various arbitrary ways chosen for the above examples.

3. RELATING A BOUNDARY-VALUE PROBLEM TO THE E-FIELD KINK MODEL

As previously mentioned, the kink model, while illustrating the E-fields of a charge in free space undergoing essentially arbitrary acceleration and motion, does not include the kinds of boundary conditions applicable to a perfect electric conductor (PEC). Thus, it seems reasonable to ask whether, and if so how, the radiation phenomena manifested by the kink model might reveal anything about radiation from a PEC?

Perhaps the most important difference between the kink model and a BV problem is that in the former the charge can move at any speed less than c while the dynamic radiation components of the field do move at light speed. On the other hand, physical charges in a real, material medium can not themselves move at light speed. Since the radiation field for such a simple straight-wire antenna as a center-fed dipole remains in contact with the antenna until its radiation sphere expands to the dipole ends, this means that fields move at light speed along the dipole's length. The associated electric field must terminate normally to the dipole's surface, and so the accompanying charge must also effectively be moving at light speed. But if physical charge can't move that fast, what is the mechanism that permits the normal E-field to be terminated at the PEC's surface? The answer seems to be that the speed of the equivalent charge, confined to the surface of the PEC, is determined by charge interaction along the wire in much the same manner as a row of falling dominoes. In the latter case, the propagation speed of a row of falling dominoes can greatly exceed the speed exhibited by each one individually.

A second question that needs consideration is how and where charge might be "wriggled" on a straight wire to cause radiation? Two obvious areas are the feed region, where the charge is subject to the applied voltage, and the wire ends where the charge is reflected and the current goes to zero. Perhaps of most interest, though, is can wriggling, and therefore the generation of radiation fields, take place anywhere else on the straight-wire dipole?

One aspect as to whether radiation does occur from along the length of a straight wire is to determine if charge can slow down or speed up there in the absence of an exciting field. Considering the above discussion, where it's deduced that the effective speed of charge along the wire must match that of the external fields it terminates, it appears that gradual slowing of the charge moving down the wire does not occur unless the electrical parameters of the external medium were to be changing. So, charge slowing can not be a cause of length-wise EM radiation from a straight wire. But might there be another kind of acceleration mechanism?

Results obtained previously by the authors using a technique called FARS (Far-field Analysis of Radiation Sources) [5,6] indicate that reflection acceleration does indeed take place along a straight wire, based on analysis done in both the time domain and frequency domain. The FARS analysis also seems consistent with previous frequency-domain work by Schelkunoff and Feldman [7] and recent results obtained in the time domain by Smith [8]. Reflection acceleration evidently is a result of the fact that the local wave impedance of a constant-radius wire varies with distance, causing a small, but significant, reflection of a propagating wave. This reflection, which occurs in both the time and frequency domains, represents an acceleration of reflected charge in an amount proportional to 2c, since that part of a wave propagating, for example, in the +x direction at speed c which is reflected then propagates in the -x direction at the same speed.

An example of a FARS result for a straight-wire dipole 10 wavelengths long is shown in Fig. 6 where the power contributed by each segment is plotted as a function of position for a normalized current magnitude. Possibly somewhat surprising is the fact that, while the expected maxima are seen in the source region and at the wire ends, there is a series of peaks between them, diminishing with distance from either region, rather than a monotonic variation. If the current/charge wave that propagates along the wire experiences a continuous partial reflection, how can that be consistent with the oscillatory nature of the linear power density seen in Fig. 6?

An answer as to why the segment power oscillates with distance in the frequency domain can be developed as follows. Note first that the current on a dipole antenna more than a wavelength long or so is a standing wave having a magnitude typified by the plot for this particular antenna in Fig. 7. But a standing wave such as shown here is comprised primarily of two oppositely propagating traveling waves (a NEC solution also exhibits a significant constant-current term near perturbations such as wire ends, feedpoints and bend). Current maxima occur where opposite-signed peaks in the charge waves coincide, and minima occur where same-signed peaks coincide (since the charge pulses are

moving in opposite directions). A comparison of Fig. 7 with Fig. 6 shows that the peaks in the latter coincide with maxima in the current magnitude. Further note that a reflection of a positive charge wave going in the +x direction produces an electric field of the same sign as reflection at the same point of a negative charge wave going in the - x direction [see Eqs. (1) and (2) below]. Since these reflection-caused E-fields are then additive, maxima in the local radiated power should be expected. On the other hand, where the current minima are found, the reflection-caused E-fields cancel because they involve reflection of same-signed charge waves in opposite directions. Consequently, minima in the local radiated power should occur at current minima and an overall oscillatory pattern is expected. Thus, the results of Fig. 6 are consistent with the standing current of Fig. 7 and a charge-reflected interpretation of the radiated fields. Note that the spatial variation of the segment powers is greater than that of the current, indicating that the charge reflection must vary to a greater degree with distance from the source and wire ends than does the current itself. It's also worth noting that the far electric field of a wire, being obtainable explicitly from a current integration, implies that incremental contributions to the far-field power will exhibit some proportionality to the local current, also in accord with the above discussion.

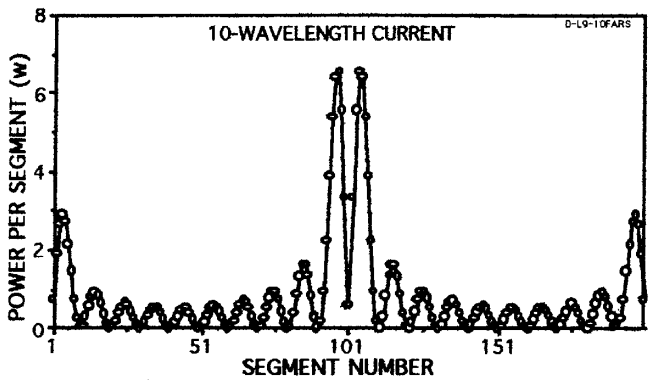

Figure 6. The segment powers obtained from FARS for a 10-wavelength long, center-fed dipole antenna.

Some results from a time-domain version of FARS (TD-FARS) are presented in Fig. 8 for a long, straight wire impulsively excited at its center by a Gaussian voltage are presented in Fig. 8, where the time-domain solution is obtained using TWTD [9]. The segment powers are computed in essentially the same fashion as used for the frequency-domain example of Fig. 6, except that now the solution is followed as a function of time. Subsequent time integration of the segment powers yields the segment energies.as shown in Fig. 8 at a succession of time steps. In one respect, the segment energies in the time domain here are similar to the segment powers in the frequency domain of Fig. 6 in that they exhibit maxima near the center and ends of the wire. The segment energies, however, monotonically decrease from each maxima, a not surprising result since there is no standing wave on the wire in the time domain analogous to that which occurs in the frequency domain. Also, these time-domain segment energies are quite similar, qualitatively at least, to some analytical work recently reported by Smith [8].

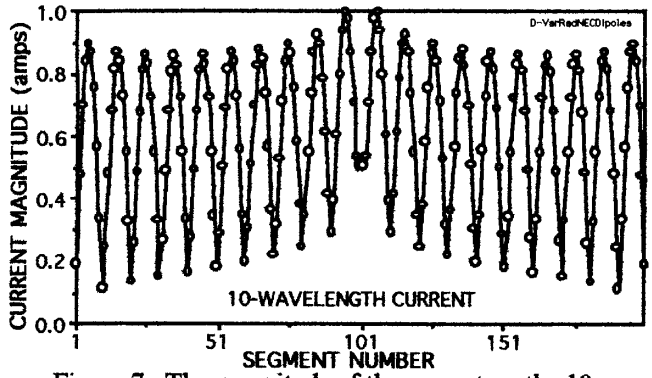

Figure 7. The magnitude of the current on the 10-wavelength dipole whose FARS results are shown in Fig. 6.

The results presented thus far are inferential with respect to how radiation is produced, both for the E-field kink model and FARS examples. In the following, an effort is made to draw a more direct connection between the radiated fields and the charge behavior on an impulsively excited wire.

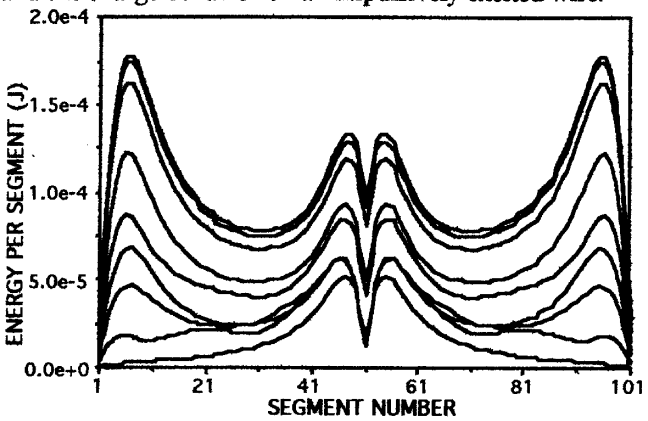

Figure 8. The segment energies as a function of position on a straight wire at several instants of time as obtained from a TWTD computation. Reading from the bottom, the time-step numbers are 50, 75, 100, 125, 175, 250, 500, 750 and 999.

4. A MORE QUANTITATIVE APPROACH USING TWTD

One potential advantage of a time-domain (TD) model is the possibility it may offer for obtaining a better understanding of EM phenomena, including the physics of radiation. It is in that spirit that in the following discussion the time variation of the broadside far electric field radiated by an impulsively excited straight wire is examined. This is done to determine whether, and how, that radiation might be related to the motion of equivalent charge on the wire, using the Lienard-Wiechert expression for the E-field as a reference, and as a continuation of the preceding discussion. Basically, an old problem is being revisited and examined

in more detail to see whether new insights might be achieved. One question to be considered, in particular, is whether such time-domain phenomena might shed any light on the question about whether straight-wire antennas radiate from anywhere else besides their ends and feedpoint.

The computer model used to obtain the following results is TWTD (Thin-Wire Time Domain) [9], which incorporates a time-dependent, thin-wire electric-field integral equation. The version used here employs a name-list input and was adapted to the Macintosh PowerPC by Burke [10]. It's compiled in double-precision Fortran and permits a maximum of 600 space samples (segments) and 1200 time steps. The TWTD code has been widely validated so it's assumed that so long as problem data is correct and the appropriate model guidelines are followed, the results are valid. The equivalent current and charge on the surface of a perfectly wire are computed as a function of space and time. In the following, it should be understood that terms current and charge will be used without further including the adjective "equivalent" before them.

The basic problem to be considered is a long, straight wire that is excited at its center by a Gaussian voltage pulse, $V = \exp[-a^2(t - t_{max})^2]$, where $a = 7.4669 \times 10^9$/s and $t_{max} = 4 \times 10^{-10}$ sec. The wire is comprised of 599 segments, has a total length of 2.0034 m, and a radius of 1 mm. A time step of 1.115×10^{-11} sec is used so that $c\Delta t = \Delta x = 0.003345$ m. A space plot of the charge density, Q, multiplied by light speed, c, is shown in Fig. 9 at several time steps together with the current at time step 301. There are two immediate observations that can be made about this plot. One is that the current and Qc are essentially identical numerically, i.e., the surface equivalent current on a long wire away from the feedpoint and ends is well approximated by its associated charge moving at the speed of light. This implies that the E- and H-fields essentially comprise a TEM field propagating along the wire, since $I = 2\pi aJ = 2\pi aH$ and $E = Q/(2\pi a\varepsilon)$, where a is the wire radius. Thus, $E/H = [Q/(2\pi a\varepsilon)]/(I/2\pi a) = Q/(\varepsilon I) = 1/(c\varepsilon) = \sqrt{(\mu\varepsilon)}/\varepsilon = \eta$, so the fields at the wire's surface where $I \sim Qc$ are related by the free space wave impedance, η. But this relationship doesn't hold at the wire ends, nor in the source region where the ratio of I to Q is much different.

The second observation is that the amplitudes of the Qc pulses decrease with distance from the feedpoint, implying some sort of energy-loss mechanism. Since the wire is modeled here as a perfect electrical conductor (PEC), the only possible loss mechanism is radiation. The question then arises about where the radiation comes from, which will be discussed further below.

That the charge is moving at essentially light speed is demonstrated in Fig. 10 where the total distance along the wire that the peak of the charge pulse has moved is plotted at intervals of 50 steps in the time-stepping solution. In this case, the 599-segment wire is excited 50 segments from one end to increase the unperturbed propagation time, where the charge peak is that of the pulse moving towards the farthest wire end. A best-fit straight line to this data has a slope of 2.9868×10^8 m/s, which is within 0.5% of c. Note also that there is no apparent change in slope of this data during the time the pulse reflects from the end of the wire, which implies that any reflection delay is short on this time scale.

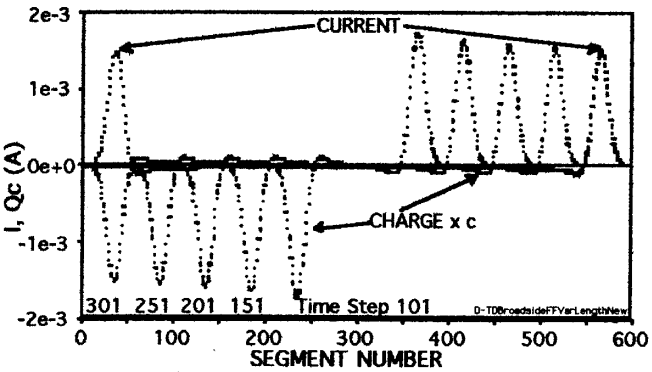

Figure 9. The current at time step 301 and charge density Q times light speed at several time steps for a long straight wire excited by a Gaussian voltage pulse at its center at segment 300.

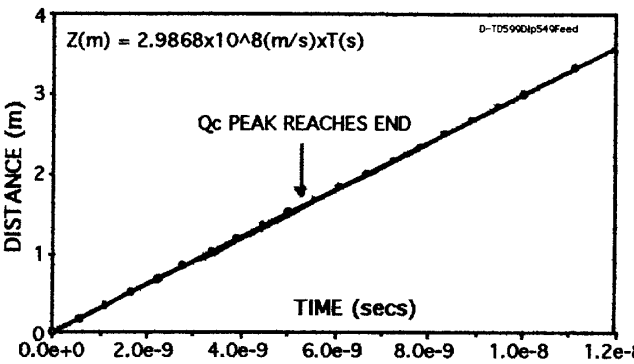

Figure 10. Distance traveled by the peak of the Qc pulse from the feedpoint of a 599-segment wire excited 50 segments from one end at intervals of 50 time steps. A best-fit straight line yields a speed of 2.9868×10^8 m/s, with no obvious perturbation occurring during end reflection.

The square of the broadside far electric fields radiated by wires of the same radius but whose length is varied by using different numbers of segments of the same length as that used for the 599-segment dipole, and excited by the same voltage pulse, are presented in Fig. 11. For clarity, the plot for each wire is shown only to the termination of its end-radiated pulse. The feedpoint radiation pulse is identical for all of the wires, of course, while the time at which the end radiation occurs is delayed by a propagation delay, with the corresponding amplitudes slightly less, as the wire length increases. In addition, there is a smaller, but continuous, radiation component between the feedpoint

and end peaks,denoted on the plot as "intermediate radiation." It seems likely that this intermediate radiation is associated with the diminution of the charge pulses as they propagate down the wire, and seems generally consistent with the FARS results above, as discussed further below.

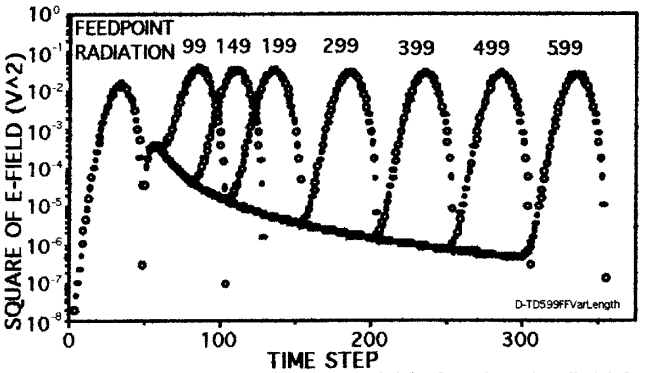

Figure 11. The square of the broadside far electric field for wires having from 99 to 599 equal-length segments and excited at their centers by a Gaussian voltage pulse. A continuous, decreasing, intermediate radiation contribution joins the feedpoint and end-radiation pulses.

Before further examining the possible cause of the intermediate radiation, it's revealing to plot the peak magnitude of the end-radiation pulse versus the peak of the sum of the absolute values of the charge pulses that reflect from the ends of the wire. First note that $q(x) = Q(x)\Delta$ is the total charge per segment, and thus the amount of charge moving per time step at a segment centered at x. The peak values of +q and - q incident on opposite ends of the wire versus the peak broadside value of $r|\mathbf{E}|$ is shown in Fig. 12, with the wire length in segments a parameter. Since the positive charge pulse reflected from the right end of the wire experiences a negative acceleration relative to that of the negative charge pulse reflecting from the left end their fields are additive, as shown by the Lienard-Wiechert expression for the far electric field, given by [1]

$$\mathbf{E} = q\{\mathbf{r}\mathbf{x}[(\mathbf{r} - \mathbf{r}\mathbf{u}/c)\mathbf{x}\mathbf{d}\mathbf{u}/dt]\}/(4\pi\varepsilon_0 c^2 s^3) \qquad (1)$$

where $\mathbf{s} = \mathbf{r} - (\mathbf{u}\cdot\mathbf{r})/c$ with $\mathbf{u}$ the velocity vector of the charge and $\mathbf{r}$ denoting the observation point. For the special case at hand where $\mathbf{r}$ is perpendicular to $\mathbf{u}$, $s = r$. Also, since the acceleration is parallel to $\mathbf{u}$ the expression for the far E-field then simplifies to

$$r\mathbf{E} = q\mathbf{d}\mathbf{u}/dt/(4\pi\varepsilon_0 c^2) \sim 10^{-7} q\mathbf{d}\mathbf{u}/dt. \qquad (2)$$

The ratio $r|\mathbf{E}|/q = 4.018\text{x}10^{12}$ provides a best straight line between $r|\mathbf{E}|$ and the total end-reflected q in Fig. 12. Using Eq. (2) this implies a value for du/dt of $\sim 4.018\text{x}10^{19}$ m/s^2. Since du is of order 2c, this further indicates that dt is in the range 1.493×10^{-11} sec. Note that a time step of $\Delta t = 1.115\text{x}10^{-11}$ sec $= \Delta x/c$ was used in the TWTD solution, suggesting that the effective reflection time is of the same order as the time step. But the magnitude of E must be independent of the model parameters. Since the charge per segment, q, is given by $q = Q\Delta x = Qc\Delta t$, then $|E| \sim 10^{-7} Qc\Delta t|du/dt| = 2\text{x}10^{-7} Qc^2 = 60Qc = 60I = 1.8\text{x}10^{10} Q$, and the model parameters do cancel out as required.

A more-detailed comparison of the broadside E-field and the end-reflected charge pulse for the asymmetrically excited dipole is shown in Fig. 13. In this case the ratio $r|\mathbf{E}|/q = 4.531\text{x}10^{12}$ normalizes the peak values of $r|\mathbf{E}|$ and q and a value for du/dt of $\sim 4.531\text{x}10^{19}$ m/s^2 results, yielding a value for dt of 1.25×10^{-11} sec. Again, this is comparable to the time step used in the numerical model.

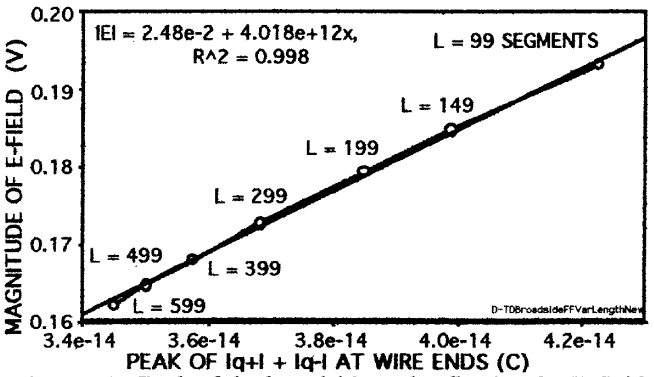

Figure 12. Peak of the broadside end-reflection far E-field as a function of the sum of the magnitudes of the charge pulses incident on each end of a straight wire of various lengths in segments, denoted by L. The relationship is essentially linear, in accord with Eq. (2) with the best-fit straight line as given.

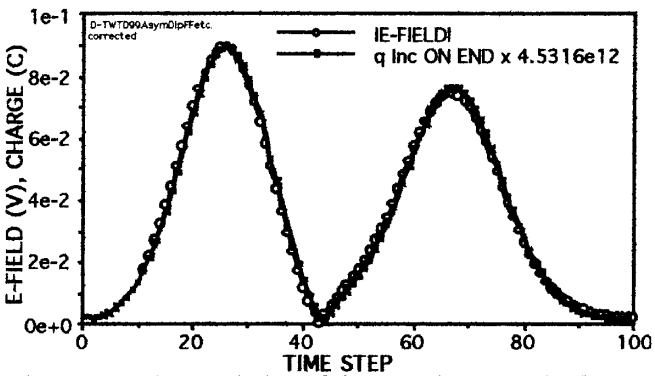

Figure 13. Time variation of the magnitudes of the far E-field and the charge pulse incident on the end of a wire dipole asymmetrically excited by a Gaussian voltage.

On turning to the possible cause of the intermediate radiation, it's instructive to examine Fig. 14 where I and Qc are shown on the right half of the 599-segment dipole on an expanded vertical scale at three times steps. In the "trailing" region behind the propagating pulses, the current and net charge, although both are negative, are quite different

numerically. Since in regions away from the feedpoint and near the ends it has been found that $I \sim Qc$, we hypothesize that their difference here indicates the negative current must be comprised of two components. One component is a positive charge reflected from the outward-moving positive Q/I pulse back towards the feedpoint. The other is due to "extraction" and rightward movement of negative charge from the feedpoint. Both comprise a negative current (the same phenomenon occurs with opposite-signed charge on the other side of the feedpoint).

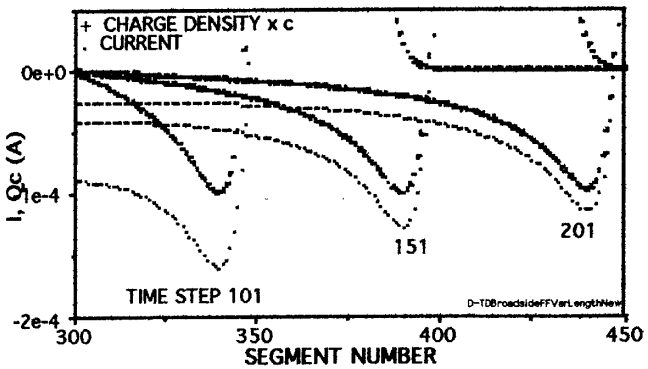

Figure 14. The trailing current (small dots) and charge density times c on the right-hand half of the 599-segment dipole at three time steps. The sign change in the current behind the outward-propagating positive pulse is apparently caused by reflection of positive charge from the pulse and negative charge from the feedpoint at segment 300. Note that the charge is an odd function and the current is an even function about the center feedpoint at segment 300.

It's possible to estimate this reflected charge in two ways. One is to integrate the outward-propagating charge pulse as a function of time, with the difference between successive time steps giving the reflected charge per time step, a rather "noisy" result. The other is to use the trailing negative current and net charge, as follows. First note that on the right-hand half of the antenna where the outgoing charge pulse is positive, the net charge density is given by

$$Q_{net} = -Q_{-,trail} + Q_{+,refl} \tag{3a}$$

so that the net current is this region becomes

$$I_{net} \sim c(-Q_{-,trail}) + (-c)Q_{+,refl}$$
$$= -c(Q_{-,trail} + Q_{+,refl}). \tag{3b}$$

The above two equations give $Q_{-,trail}$ and $Q_{+,refl}$ as

$$Q_{+,refl} = (cQ_{net} - I_{net})/2c \tag{4a}$$
$$Q_{-,trail} = (cQ_{net} + I_{net})/2c. \tag{4b}$$

The charge densities, $Q_{-,trail}$ and $Q_{+,refl}$ in Eq. (4), are computed, respectively, one segment to the right of the feedpoint and immediately behind, or to the left, of the rightward-moving pulse. This is done to obtain these quantities at the point where the acceleration occurs.

Results from both approaches are plotted in Fig. 15. The RMS difference between them is normalized to the peak charge density is about 3%. The near equality of these two independent ways of computing the reflected charge supports the hypothesis made above that the trailing negative current is indeed comprised of positive and negative charge moving in opposite directions. It should be noted that, in computing the reflected and trailing charges here, higher-order reflections are not taken into account.

Now assume that the acceleration times for $q_{-,trail}$ (given by $Q_{-,trail}\Delta x$) and $q_{+,refl}$ ($Q_{+,refl}\Delta x$) are equal while noting that du for the latter is twice that of the former. Thus

$$r|E| \approx 10^{-7}|[q_{trail}du_{trail}/dt + q_{refl}du_{refl}/dt]|$$
$$= 10^{-7}[q_{trail} + 2q_{refl}]|du/dt|. \tag{5}$$

A plot of the broadside intermediate E-field is compared with the total (on both halves of the antenna) absolute reflected and trailing charge in Fig. 16. They agree within a few per cent, implying that the intermediate radiation in Fig. 10 appears to be caused both by reflection of outward-propagating charge and extraction of opposite-signed charge from the source region. The reflection phenomenon supports the interpretation that radiation does indeed occur from along the length of a wire antenna, the question that motivated this section of the article. Since both $q_{-,trail}$ and $q_{+,refl}$ exhibit very similar time variations, however, a different weighted combination other than in Eq. (5) could yield similar results, albeit with a different implied value for dt.

The value for dt implied by Fig. 16, assuming the reflected charge undergoes a du of 2c while the trailing charge has a du of c, is $1.82\text{x}10^{-11}$ sec. The values for dt estimated from the three different phenomena explored above differ by a factor of about 50% with an average value of $1.22\text{x}10^{-11}$ sec.

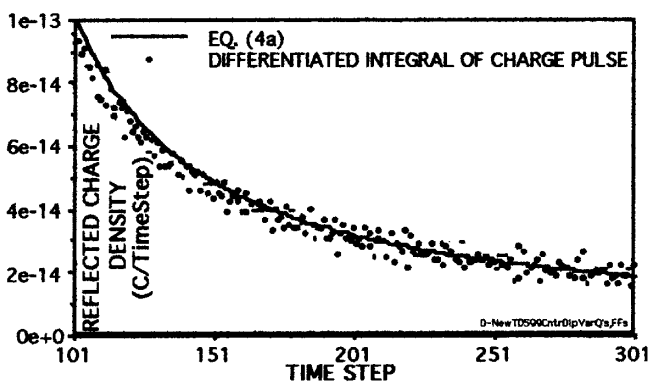

Figure 15. The reflected charge from integrating the outgoing charge pulse and using Eq. (4a). The noisy appearance is caused by subtracting two nearly equal numbers.

CONCLUDING REMARKS

Three different perspectives of electromagnetic radiation have been explored here. The E-field kink model demonstrates in a very straightforward way that "wriggling" a charge causes its field lines to wriggle similarly, producing propagating kinks that constitute radiation. A technique called FARS, that employs a slightly different way of analyzing the far field, provides an alternate way to quantitatively determine the origin of radiated power from over a perfectly conducting surface. Finally, the current and charge flowing on an impulsively excited thin wire was carefully examined and correlated with the broadside far field. It's clear that charge acceleration in the source region and end reflection is the predominate cause of radiation. The hypothesis that a partial-reflection phenomenon causes radiation to occurs from all along the wire is supported by more detailed analysis of the current and charge behavior behind the outward-propagating Q/I pulse. In addition, it appears that radiation continues from the feedpoint even after the exciting voltage goes to zero due to opposite-signed charge extracted from it. When examined at broadside, these various radiation phenomena seem to be in semi-quantitative agreement with the Lienard-Wiechert potentials, providing a feasible link between an accelerated-charge analysis and an equivalent source, boundary-value model of electromagnetic radiation. Further investigation is needed, however, to make a more convincing quantitative connection between them.

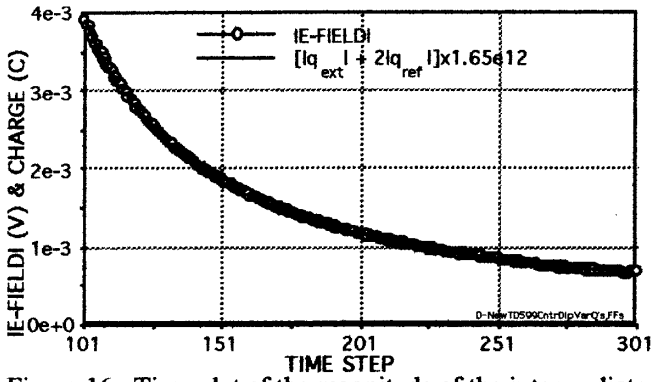

Figure 16. Time plot of the magnitude of the intermediate broadside far E-field and total reflected and extracted charge for the center-excited 599-segment dipole. Reflected charge is multiplied by 2 to account for the 2c speed change it experiences relative to the trailing charge.

REFERENCES

1. W. K. H. Panofsky and M. Phillips, *Classical Electricity and Magnetism*, Addison-Wesley Publishing Co., Inc., Cambridge, MA, 1955.

2. Blas Cabrera, Physics Simulations II: Electromagnetism, Academic Version," Intellimation Library for the Macintosh, PO Box 1530, Santa Barbara, CA 93116-1530, 1990.

3. G. S. Smith, *Classical Electromagnetic Radiation*, Cambridge University Press, 1997.

4. J. J. Thomson, *Electricity and Matter*, Charles Scribner's Sons, New York, 1904.

5. E. K. Miller, PCs for AP and Other EM Reflections, *IEEE AP-S Magazine*, Vol. 41, No. 2, April, pp. 82-86; Vol. 41, No. 3, June, pp. 83-88, 1999.

6. E. K. Miller and G. J. Burke, "Time-Domain Far-Field Analysis of Radiation Sources," *IEEE International Symposium on Antennas and Propagation Digest*, Salt Lake City, UT, Hilton Hotel, July 16-21, pp. 1546-49, 2000.

7. S. A. Schelkunoff and C. B. Feldman, "On Radiation from Antennas," *Proceedings of the IRE*, Vol. 30, pp. 511-516, 1942.

8. G. S. Smith and T. W. Hertel, "On the Radiation of Energy from Simple Current Distributions," to appear in the *IEEE Antennas and Propagation Society Magazine*.

9. J. A. Landt, E. K. Miller, and M. L. Van Blaricum, *WT-MBA.LL1B: A Computer Program for the Time-Domain Response of Thin-Wire Structures*, Lawrence Livermore Laboratory, Livermore, CA, UCRL-51585, 1974.

10. G. J. Burke, Private Communication, 1991.

11. S. Castillo, "The Interpretation of Body Current Distributions in Designing Low-RCS Scatterers," 1997 North American Radio Science Meeting, Montreal, Canada, p. 736.

12. H. E. Green, "Fundamentals of Radiation from Antennas," Symposium Digest, p. 17, Seventh Australian Symposium on Antennas, CSIRO, Sydney, Australia, February, 2001.

APPENDIX: THE FARS APPROACH

FARS can be implemented in either the frequency domain or the time domain. As an alternative to imaging using the bistatic far fields, as described by Shaeffer et al. (1997), however, FARS seeks instead to determine the contribution made to the total power flow in the far field by each incremental source, or segment in a moment-method sense, on the wire boundary. The FARS power, $P_{i,FARS}$, for segment s_i is thus given by

$$P_{i,FARS} = \frac{\lim r\to\infty r^2}{2\eta}\int_0^{\pi}\int_0^{2\pi} (\mathrm{Re}[\mathbf{e}_i(\theta,\varphi)\cdot\mathbf{E}^*(\theta,\varphi)])\sin\theta d\theta d\varphi \qquad (A1)$$

where $\mathbf{e}_i(\theta,\varphi)$ is the partial far electric field due to the source on segment i, $\mathbf{E}(\theta,\varphi)$ is the total far electric field for the N source segments, and η is the medium impedance.

Upon dividing $P_{i,FARS}$ by the segment length Δ_i, a quantity denoted here as the "linear power density," or LPD, is obtained at the center of segment s_i. The total radiated power can then be found from integrating the LPD over the entire object, which, by definition, must equal the usual result for the radiated power. Equivalently, the $P_{i,FARS}$ values can be summed over all segments to yield the total radiated power.

In essence, the orders of the spatial and angle integrations involved in computing the usual radiated power have been interchanged, to obtain the intermediate quantity coming from doing the angle integration first as given in Eq. (A1). The quantities in Eq. (A1) are time-harmonic in the frequency domain and time-dependent in the time domain where the fields are by sampling as a function of observation time. In the latter case, a time integral of the instantaneous power up to time T yields the total energy as a function of time. Note that the FARS computation differs from a conventional evaluation of the total far-field power only in defining the intermediate quantity $P_{i,FARS}$. Also, although there is no constraint that each $P_{i,FARS}$ be positive, the physical significance of negative values may be unclear at this point and is discussed elsewhere [5, 6].

Castillo [11] described a somewhat-similar approach, wherein a total far-field power value is computed using the incremental fields of all but segment i, with i sequentially scanned over the entire object. Since the fields are additive, but the incremental powers are not, the result obtained only approximates the total radiated power.